Lifshitz-type formulas for graphene and single-wall carbon nanotubes: van der Waals and Casimir interactions

M. Bordag, B. Geyer, G. L. Klimchitskaya,* and V. M. Mostepanenko†
Center of Theoretical Studies and Institute for Theoretical Physics, Leipzig University, Augustusplatz 10/11, D-04109 Leipzig, Germany

Lifshitz-type formulas are obtained for the van der Waals and Casimir interaction between graphene and a material plate, graphene and an atom or a molecule, and between a single-wall carbon nanotube and a plate. The reflection properties of electromagnetic oscillations on graphene are governed by the specific boundary conditions imposed on the infinitely thin positively charged plasma sheet, carrying a continuous fluid with some mass and charge density. The obtained formulas are applied to graphene interacting with Au and Si plates, to hydrogen atoms and molecules interacting with graphene, and to single-wall carbon nanotubes interacting with Au and Si plates. The generalizations to more complicated carbon nanostructures are discussed.

PACS numbers: 73.22.-f, 34.50.Dy, 12.20.Ds

I. INTRODUCTION

It has been known that two neutral atoms or molecules separated by a distance which is rather small but much larger than the atomic dimensions interact through the van der Waals force. As was shown by London, the van der Waals force arises in second order perturbation theory from the dipole-dipole interaction. It is caused by the dispersions of dipole operators, i.e., by quantum fluctuations [1]. Being a quantum phenomenon, it depends on the Planck constant $\hbar$. In consequence of interatomic interactions, the van der Waals force acts also between an atom and a macroscopic body and between two closely spaced macroscopic bodies. If the separation between two atoms, an atom and a macroscopic body or between two macrobodies is sufficiently large, so that the retardation of the electromagnetic fluctuating interaction contributes significantly, the van der Waals force depends on both $\hbar$ and the velocity of light c. In this regime the force is usually labeled as Casimir [2] or (in the case of atom-atom or atom-wall interaction) Casimir-Polder [3] force. Van der Waals and Casimir forces play an important role in the interaction of a single layer of graphite (hereafter, graphene) with macroscopic bodies (a material plate or a semispace) and with microparticles (an atom or a molecule). The physics of interactions between graphene and carbon nanostructures [4] with macroscopic bodies and microparticles is significant for the understanding of layered systems, bundles of nanotubes or metallic nanowires and absorption phenomena. Special attention was attracted to this problem after the proposal of Ref. [5] to use the single-wall carbon nanotubes for the purposes of hydrogen storage. Subsequently controversial results on this subject were obtained [6]. Especially, the microscopic mechanisms underlying the absorption phenomenon remain unclear.

Theoretically the interaction of hydrogen atoms with graphite sheets and carbon nanotubes has been studied in Ref. [7] using the density functional theory and in Refs. [8, 9] using the nonrelativistic perturbation theory for degenerate levels of a two-level atomic system. The adsorption of fullerene molecules on graphite was considered in Ref. [10] demonstrating that the interaction is basically proportional to the number of neighboring atoms. Most of theoretical work on the van der Waals force in layered structures and between carbon nanotubes was done using the density functional theory [11, 12, 13, 14, 15, 16]. It is known, however, that in some cases density functional theory (especially when used with linear-density approximation) gives not enough precise description of van der Waals interactions [17]. In Ref. [18] the Lifshitz theory of the van der Waals and Casimir force was extended to the case of a microparticle interacting with a plane surface of an uniaxial crystal and with a multi-wall carbon nanotube. It was shown that the position of a hydrogen atom inside the multi-wall carbon nanotube is energetically preferable as compared to the outside position.

It is common knowledge that the Lifshitz theory [19, 20] provides the fundamental description of the van der Waals and Casimir interaction between two macroscopic bodies and between a microparticle and a macroscopic body. In the framework of this theory the interaction energy and the force are expressed in terms of the dielectric permittivity of

* On leave from North-West Technical University, St.Petersburg, Russia.
† On leave from Noncommercial Partnership "Scientific Instruments", Moscow, Russia.

macrobodies or the dynamic polarizability of a microparticle. Recently, the Lifshitz theory was successfully applied to the interpretation of precision measurements of the Casimir force [21, 22, 23, 24, 25] and to the calculation of atom-wall interaction in connection with Bose-Einstein condensation [26, 27]. In Ref. [18] the Lifshitz theory was adapted for the case of sufficiently thick multi-wall carbon nanotubes using the idealized description of the wall material by dielectric permittivity. This idealization is, however, not applicable for the description of single-wall nanotubes which narrows the applicability of the standard Lifshitz theory.

In the present paper we use the description of graphene in terms of the two dimensional free electron gas [28] in order to extend the Lifshitz theory of the van der Waals and Casimir interaction to the case of carbon systems. Graphene is considered as an infinitesimally thin positively charged flat sheet, carrying a continuous fluid with some mass and negative charge densities. This sheet is characterized by some typical wave number Ω determined by the parameters of the hexagonal structure of graphite. In Refs. [29, 30] the interaction of the electromagnetic oscillations with such sheet was considered and the normal modes and reflection coefficients were found. The van der Waals and Casimir interaction between the two parallel plasma sheets was described in Ref. [31] using a Lifshitz-type formula. The important distinctive feature of this formula is that it does not use the concept of the dielectric permittivity of the sheet.

Here we obtain Lifshitz-type formulas for the van der Waals and Casimir interaction of graphene and material semispace or a plate. In so doing the semispace or the plate are described using the dielectric permittivity and graphene is considered as a plasma sheet. The numerical computations of the interaction energy and the force acting between graphene and thick plates made of different materials are performed. The Lifshitz-type formula for the interaction of graphene with a microparticle (an atom or a molecule) is also obtained. This formula is applied to the computations of the interaction of graphene with hydrogen atoms and molecules. The approximate formulas for the interaction of a single-wall carbon nanotube with a material plate are presented when the nanotube is in close proximity or far away from the plate.

The paper is organized as follows. In Sec. II the Lifshitz-type formulas are obtained for the interaction of graphene with a semispace or a plate. Sec. III contains the results of numerical computations using these formulas for metal and dielectric plates. In Sec. IV the interaction of graphene with a hydrogen atom or a molecule is considered. Sec. V is devoted to the interaction of a single-wall carbon nanotube with a metal or dielectric plate. Sec. VI contains our conclusions and discussion.

II. INTERACTION OF A GRAPHENE WITH A SEMISPACE OR A PLATE

We consider the van der Waals and Casimir interaction of a graphene occupying the xy-plane, $z=0$, with a material semispace or a plate of thickness d. The separation distance between the boundary plane of the semispace (plate) and graphene is a. The dispersion interaction of the two plane parallel bodies (plates or semispaces) labeled by the upper indices 1 and 2 with the electromagnetic oscillations can be described in terms of the reflection coefficients $r^{(1)}_{\rm TM,TE}$ and $r^{(2)}_{\rm TM,TE}$ for two independent polarizations of electromagnetic field (transverse magnetic and transverse electric). In so doing the van der Waals and Casimir interaction energy per unit area is given by the Lifshitz formula [19, 20, 21]

$$E(a)=\frac{\hbar}{4\pi^2}\int_0^\infty k_\perp dk_\perp\int_0^\infty d\xi\left[\ln\left(1-r^{(1)}_{\rm TM}r^{(2)}_{\rm TM}e^{-2aq}\right)\right.$$
$$\left.+\ln\left(1-r^{(1)}_{\rm TE}r^{(2)}_{\rm TE}e^{-2aq}\right)\right]. \tag{1}$$

Here $k_\perp$ is the magnitude of the wave vector component perpendicular to the z-axis (i.e., lying in the plane of the plates), ξ is the frequency variable along the imaginary axis ($\omega=i\xi$), and

$$q=\sqrt{k_\perp^2+\frac{\xi^2}{c^2}}. \tag{2}$$

Equation (1) is applicable at not very high temperatures (not too large separations). As an example, at room temperature ($T=300\,{\rm K}$) thermal corrections to Eq. (1) are negligible up to separations of about $1\,\mu$m. If the temperature is higher (separation is larger) Eq. (1) is simply generalized by changing the integration with respect to ξ for the summation over the discrete Matsubara frequencies. The general derivation of Eq. (1) for arbitrary reflection coefficients can be found in Ref. [21].

The commonly accepted approach (see, e.g., [19, 20, 21, 22, 23, 24, 25, 26, 27]) uses the Fresnel reflection coefficients of the semispaces and plates expressed in terms of the frequency-dependent dielectric permittivities. Let the semispace

labeled 2 be made of isotropic material and be described by the dielectric permittivity $\varepsilon(\omega)$. In this case the reflection coefficients are [19, 20, 21, 22, 23, 24, 25]

$$r_{\rm TM}^{(2)} \equiv r_{\rm TM,s}^{(2)}(\xi,k_\perp) = \frac{\varepsilon(i\xi)q-k}{\varepsilon(i\xi)q+k},$$
$$r_{\rm TE}^{(2)} \equiv r_{\rm TE,s}^{(2)}(\xi,k_\perp) = \frac{k-q}{k+q}, \tag{3}$$

where

$$k=\sqrt{k_\perp^2+\varepsilon(i\xi)\frac{\xi^2}{c^2}}.$$

If the second body is a plate of finite thickness d, Eq. (3) should be replaced by [18]

$$r_{\rm TM}^{(2)} \equiv r_{\rm TM,p}^{(2)}(\xi,k_\perp) = \frac{\varepsilon^2(i\xi)q^2-k^2}{\varepsilon^2(i\xi)q^2+k^2+2qk\varepsilon(i\xi)\coth(kd)},$$
$$r_{\rm TE}^{(2)} \equiv r_{\rm TE,p}^{(2)}(\xi,k_\perp) = \frac{k^2-q^2}{k^2+q^2+2qk\coth(kd)}. \tag{4}$$

If the first body is also a semispace or a plate, its reflection coefficients are obtained from Eqs. (3) and (4) by the replacement of the upper indices 2 for 1.

In our case the first body is graphene and it cannot be described macroscopically it terms of the dielectric permittivity. The van der Waals and Casimir interaction of a semispace or a plate made of isotropic material with the graphite plate containing a few hexagonal layers was considered in Ref. [18] using the reflection coefficients for a uniaxial crystal. In the case of a graphite plate of thickness d they take the form

$$r_{\rm TM}^{(1)} \equiv r_{\rm TM,p}^{(1)}(\xi,k_\perp)$$
$$= \frac{\varepsilon_x(i\xi)\varepsilon_z(i\xi)q^2-k_z^2}{\varepsilon_x(i\xi)\varepsilon_z(i\xi)q^2+k_z^2+2qk_z\sqrt{\varepsilon_x(i\xi)\varepsilon_z(i\xi)}\coth(k_zd)},$$
$$r_{\rm TE}^{(1)} \equiv r_{\rm TE,p}^{(1)}(\xi,k_\perp) = \frac{k_x^2-q^2}{k_x^2+q^2+2qk_x\coth(k_xd)}, \tag{5}$$

where $\varepsilon_x(\omega)=\varepsilon_y(\omega)$ and $\varepsilon_z(\omega)$ are the graphite dielectric permittivities in the directions x,y and z, respectively, and

$$k_x=\sqrt{k_\perp^2+\varepsilon_x(i\xi)\frac{\xi^2}{c^2}}, \quad k_z=\sqrt{k_\perp^2+\varepsilon_z(i\xi)\frac{\xi^2}{c^2}}. \tag{6}$$

The number of layers in the graphite plate should be sufficiently large that the macroscopic description in terms of the dielectric permittivities is applicable.

The reflection coefficients for a sheet of graphene cannot be obtained from Eq. (5) in the limit $d\to 0$ [in fact, the coefficients (5) go to zero when d vanishes]. The reason is that the case of "thin" plate implies that d/a is sufficiently small, whereas d should be large enough for the validity of the macroscopic description in terms of ε. In Sec. III the correlation between the macroscopic description of a graphite plate by means of Eq. (5) and the case of graphene will be clarified.

A single plane hexagonal layer of graphite, i.e., graphene, can be described as infinitely thin plasma sheet where the π-electrons are treated as a continuously charged fluid moving in an immobile, overall neutralizing background of positive charge. These plasma sheets have been considered in Ref. [28] and, more recently, by Barton [29, 30] in connection with the Casimir effect for a fullerene and for a single base plane from graphite. In Ref. [31] they were used to calculate the van der Waals and Casimir interaction between the two parallel graphenes and a Lifshitz-type formula was obtained for their interaction energy.

The plasma sheet model assumes the π-electrons of the carbon atoms to be described by a negatively charged fluid confined to a plane and having the two dimensional displacement vector $\boldsymbol{R}(x,y)\exp(-i\omega t)$, where we introduced at once the usual harmonic time dependence. (In [29, 30] this vector is denoted by ξ and the wave number of the sheet Ω by q.) The fluid has a surface charge density ne and a surface mass density nm where e and m are the electron charge and mass, respectively. For the hexagonal structure of carbon layers there is one π-electron per atom [32] resulting in two π-electrons per one hexagonal cell. This leads to

$$n=\frac{4}{3\sqrt{3}l^2}, \tag{7}$$

where $l = 1.421$ Å is the side length of a hexagon.

The fluid provides a source for the Maxwell equations with surface charge and surface current densities,

$$\sigma = -ne\nabla_t \cdot \boldsymbol{R}, \quad \boldsymbol{j} = -i\omega ne\boldsymbol{R}, \tag{8}$$

where the operator ∇_t acts in the tangential direction to the sheet [here and below σ, $\boldsymbol{j}$ and fields $\boldsymbol{E}$ and $\boldsymbol{B}$ depend on coordinates; their dependence on time is obtained through the multiplication by the common factor $\exp(-i\omega t)$]. The Maxwell equations read

$$\begin{aligned} &\nabla \cdot \boldsymbol{E} = 4\pi\sigma\delta(z), \quad \nabla \times \boldsymbol{E} - \frac{i\omega}{c}\boldsymbol{B} = 0, \\ &\nabla \cdot \boldsymbol{B} = 0, \quad \nabla \times \boldsymbol{B} + \frac{i\omega}{c}\boldsymbol{E} = \frac{4\pi}{c}\boldsymbol{j}\delta(z). \end{aligned} \tag{9}$$

By the integration of Maxwell equations across the sheet, we obtain the matching conditions on the tangential and normal components of the fields [30],

$$\begin{aligned} &\boldsymbol{E}_{t,2} - \boldsymbol{E}_{t,1} = 0, \quad E_{z,2} - E_{z,1} = 2\Omega\frac{c^2}{\omega^2}\nabla_t \cdot \boldsymbol{E}_t, \\ &B_{z,2} - B_{z,1} = 0, \quad \boldsymbol{B}_{t,2} - \boldsymbol{B}_{t,1} = -2i\Omega\frac{c}{\omega}\boldsymbol{z} \times \boldsymbol{E}_t. \end{aligned} \tag{10}$$

Here $\boldsymbol{z} = (0,\, 0,\, 1)$ is the unit vector pointing in z-direction,

$$\Omega = 2\pi\frac{ne^2}{mc^2} = 6.75 \times 10^5\,\mathrm{m}^{-1} \tag{11}$$

and n is defined in Eq. (7). The quantity Ω is the main characteristic of graphene in the model under consideration. The value in Eq. (11) corresponds to the frequency $\omega_\Omega = c\Omega = 2.02 \times 10^{14}\,\mathrm{rad/s}$ (as compared, for instance, to the plasma frequency of gold $\omega_p = 1.37 \times 10^{16}\,\mathrm{rad/s}$).

We remark that now the matching conditions (10) together with the Maxwell equations (9) outside the surface, i.e., without the delta functions on the right-hand sides, provide the complete description of the interaction of the electromagnetic field with the plasma sheet. This implies, for instance, that all components of the field satisfy the usual Poisson equations,

$$\left(\Delta + \frac{\omega^2}{c^2}\right)\boldsymbol{E} = 0, \quad \left(\Delta + \frac{\omega^2}{c^2}\right)\boldsymbol{B} = 0. \tag{12}$$

After the separation of variables x and y in Eqs. (10) and (12) we arrive at a one-dimensional scattering problem in the z-direction [21]. The solution of this problem leads to the following reflection coefficients on the graphene plasma sheet taken at the imaginary frequency axis [30],

$$\begin{aligned} r_{\mathrm{TM}}^{(1)} &\equiv r_{\mathrm{TM,g}}^{(1)}(\xi, k_\perp) = \frac{c^2 q\Omega}{c^2 q\Omega + \xi^2}, \\ r_{\mathrm{TE}}^{(1)} &\equiv r_{\mathrm{TE,g}}^{(1)}(\xi, k_\perp) = \frac{\Omega}{\Omega + q}. \end{aligned} \tag{13}$$

Equations (1) and (3), (13) or, alternatively, (1) and (4), (13) allow to calculate the energy of the van der Waals and Casimir interaction between a graphene and a semispace or a plate made of some usual material described by the dielectric permittivity $\varepsilon(\omega)$. From Eq. (1) it is easy to obtain the Lifshitz-type formula for the van der Waals and Casimir force per unit area acting between graphene and material semispace or a plate,

$$\begin{aligned} F(a) = -\frac{\partial E(a)}{\partial a} = -\frac{\hbar}{2\pi^2}\int_0^\infty qk_\perp dk_\perp \int_0^\infty d\xi \\ \times \left(\frac{r_{\mathrm{TM}}^{(1)} r_{\mathrm{TM}}^{(2)}}{e^{2aq} - r_{\mathrm{TM}}^{(1)} r_{\mathrm{TM}}^{(2)}} + \frac{r_{\mathrm{TE}}^{(1)} r_{\mathrm{TE}}^{(2)}}{e^{2aq} - r_{\mathrm{TE}}^{(1)} r_{\mathrm{TE}}^{(2)}}\right). \end{aligned} \tag{14}$$

Equations (1) and (14) can be used to obtain the interaction energy and the force between an atom (molecule) and a graphene sheet (see Sec. IV) and between a carbon nanotube and a material wall (Sec. V). In the next section these equations are applied to compute the interaction of graphene with metal and dielectric walls made of real materials.

III. COMPUTATIONS OF THE VAN DER WAALS AND CASIMIR INTERACTION BETWEEN GRAPHENE AND METAL OR DIELECTRIC PLATE

Here we apply Eqs. (1) and (14) to calculate the van der Waals and Casimir interaction energy and force acting between graphene and thick plates (semispaces) made of different materials. The reflection coefficients $r^{(1)}_{\rm TM,TE}$ for graphene are given in Eq. (13), and the reflection coefficients $r^{(2)}_{\rm TM,TE}$ for a semispace are presented in Eq. (3). All parameters in Eq. (13) are specified. As to Eq. (3), it depends on the dielectric permittivity along the imaginary frequency axis. In our computations we consider metal and dielectric semispaces made of Au and high resistivity Si, respectively. High precision results for the dielectric permittivities of these materials along the imaginary frequency axis were obtained in Ref. [33] by means of the Kramers-Kronig relation

$$\varepsilon(i\xi)=1+\frac{2}{\pi}\int_0^\infty d\omega\frac{\omega{\rm Im}\varepsilon(\omega)}{\omega^2+\xi^2}. \tag{15}$$

The imaginary part of the dielectric permittivities at real frequencies was taken from the tabulated optical data [34].

The computational results for the van der Waals and Casimir energy density $E(a)$ normalized to the Casimir energy density in the configuration of the ideal metal plates,

$$E_0(a)=-\frac{\pi^2}{720}\,\frac{\hbar c}{a^3}, \tag{16}$$

are shown in Fig. 1(a) as a function of separation. The solid and dashed lines are related to the interaction of graphene with Au and Si, respectively. In Fig. 1(b) the analogous results for the van der Waals and Casimir force per unit area $F(a)$ normalized to the force per unit area,

$$F_0(a)=-\frac{\pi^2}{240}\,\frac{\hbar c}{a^4}, \tag{17}$$

acting between ideal metals are presented.

As is seen in Fig. 1, both the relative interaction energy and force between graphene and Au are greater than between graphene and Si at all separations. With the decrease of separation these quantities decrease. This is because $E(a)$ and $F(a)$ go to infinity more slowly than the respective dependencies for ideal metals in Eqs. (16) and (17). As a result, at the shortest separation indicated in Fig. 1 ($a=3\,$nm) $E/E_0=0.0252$, $F/F_0=0.0203$ for Au and $E/E_0=0.0212$, $F/F_0=0.0170$ for Si. Note that at separations less than 1–2 nm the used model of graphene as a plasma sheet may become inapplicable because it does not take the atomic structure into account. With the increase of separation up to $1\,\mu$m the interaction energy between graphene and Au achieves almost one half of that between ideal metals and the force magnitude is larger than 0.43 of that in the case of ideal metals.

Now we compare the above numerical results for Au with the analytic calculations in the asymptotic region of short separations. The dielectric permittivity of Au along the imaginary frequency axis can be approximated by means of the plasma model,

$$\varepsilon(i\xi)=1+\frac{\omega_p^2}{\xi^2}, \tag{18}$$

where ω_p is the plasma frequency. At short separations only the TM mode in Eq. (1) contributes essentially to the van der Waals energy [20]. Introducing the dimensionless variables $v=aq$ and $\zeta=a\xi/c$ and substituting Eq. (18) in Eq. (3), we rewrite the TM contribution to Eq. (1) in the following way:

$$\begin{aligned} &E(a)=E_0(a)f(\alpha,\beta), \\ &f(\alpha,\beta)=-\frac{180}{\pi^4}\int_0^\infty vdv\int_0^v d\zeta \\ &\qquad\times\ln\left[1-\frac{\alpha v}{\alpha v+\zeta^2}\,\frac{\left(1+\frac{\beta^2}{\zeta^2}\right)v-\sqrt{\beta^2+v^2}}{\left(1+\frac{\beta^2}{\zeta^2}\right)v+\sqrt{\beta^2+v^2}}\,e^{-2v}\right]. \end{aligned} \tag{19}$$

Here, $E_0(a)$ was defined in Eq. (16) and the two parameters are $\alpha=\Omega a$ and $\beta=\omega_p a/c$. Instead of the variable ζ we introduce the variable $\eta=\zeta/(\beta v)$. This brings the correction factor f in Eq. (19) to the form

$$f(\alpha,\beta)=-\frac{180\beta}{\pi^4}\int_0^\infty v^2dv\int_0^{1/\beta}d\eta \tag{20}$$
$$\times\ln\left[1-\frac{e^{-2v}}{1+\frac{v\eta^2}{t}}\frac{\left(1+\frac{1}{v^2\eta^2}\right)v-\sqrt{\beta^2+v^2}}{\left(1+\frac{1}{v^2\eta^2}\right)v+\sqrt{\beta^2+v^2}}\right],$$

where $t\equiv\alpha/\beta^2$. At short separations the parameters α and β are small (at the shortest separation $a=3\,\mathrm{nm}$ it holds $\alpha=2.02\times10^{-3}$, $\beta=0.137$). It is easily seen that only small values of η give the major contribution to the integral with respect to η in Eq. (20). Because of this, without loss of accuracy, one can replace the upper limit $1/\beta$ for ∞. Expanding the integrand in Eq. (20) in powers of β, one arrives at

$$f(\alpha,\beta)=\beta h_0(t)+\beta^3h_1(t)+\ldots, \tag{21}$$

where

$$h_0(t)=-\frac{180}{\pi^4}\int_0^\infty v^2dv\int_0^\infty d\eta \tag{22}$$
$$\times\ln\left[1-\frac{e^{-2v}}{\left(1+\frac{v\eta^2}{t}\right)(1+2v^2\eta^2)}\right].$$

Notice that the term of order β^3 on the right-hand side of Eq. (21) and the respective terms originating from the TE contribution to Eq. (1) are small at short separations and can be neglected. The parameter $t=\alpha/\beta^2$ is small and decreases with the increase of separation starting from the largest value of $t=0.108$ at the shortest separation $a=3\,\mathrm{nm}$. In Fig. 2 the values of h_0 are plotted as a function of t.

As a result, the asymptotic representation of the van der Waals interaction energy between a graphene and an Au semispace at short separations is given by

$$E(a)=E_0(a)\frac{\omega_pa}{c}\,h_0\left(\frac{\Omega c^2}{\omega_p^2a}\right). \tag{23}$$

The comparison of Eq. (23) with the results of numerical computations in Fig. 1(a) (solid line) shows good agreement in the limits of 3% within the separation region from 15 to 80 nm. At the shortest separation of 3 nm the error of the representation (23) achieves 11.5% if to compare with the computational results using the tabulated optical data. At the same time, within the separation region from 3 to 40 nm, Eq. (23) is in agreement with the numerical computations using the plasma model (18) up to a maximal error of 3%. A few computational results are presented in Table 1. Column 1 contains separation distances, and in columns 2, 3 and 4 the values of the correction factor $E(a)/E_0(a)$ are contained computed by using the tabulated optical data, the plasma model dielectric function and the asymptotic representation (23), respectively.

Note that the asymptotic expression (23) at short separations contains the velocity of light, i.e., is relativistic. This is different from the van der Waals interaction at short separations of two bodies described by the dielectric permittivity [20] but is in accordance with the short separation interaction of the two plasma sheets considered in Ref. [31].

It is instructive to consider the relationship between the graphene described by the model of a plasma sheet and the thin graphite plate containing a few hexagonal layers. For this purpose we compare the computed above interaction energy of graphene and Au semispace with the interaction of a graphite plate of some thickness d and the same semispace. The latter is computed using Eq. (1) with the reflection coefficients (3) and (5). The dielectric permittivities of graphite along the imaginary frequency axis $\varepsilon_{x,y}(i\xi)$ and $\varepsilon_z(i\xi)$ were computed in Ref. [18] by means of the Kramers-Kronig relations using the tabulated optical data for graphite from Ref. [34]. Here we use the results of that computations.

In Fig. 3 the interaction energy density of the graphite plate and Au semispace normalized for the case of ideal metals in Eq. (16) is plotted as a function of the relative plate thickness d/a at separations $a=1$, 0.5, 0.3, 0.1, and $0.05\,\mu$m (lines 1, 2, 3, 4, and 5, respectively). As is seen in Fig. 3, the magnitudes of E/E_0 decrease when $d/a\to0$. This is in accordance with Eq. (5) for the reflection coefficients which go to zero when d vanishes. From this it follows that the graphene cannot be obtained from the macroscopic plate in the limit of zero thickness. There is, however, some relationship between the cases of graphene and the graphite plate. To trace it let us plot the values of graphene-Au

relative interaction energy at separations 1, 0.5, 0.3, 0.1, and 0.05 μm from Fig. 1(a) (the solid line) on the vertical axis in Fig. 3 and draw the tangents to the respective lines $1, 2, 3, 4$, and 5. It is seen that all tangents intersect with lines 1, ... , 5 in the region $d/a \sim 0.13 - 0.18$. These values of the relative thickness are in fact characteristic for the graphite plates could be treated macroscopically in terms of the dielectric permittivity. As an example, at a separation of 50 nm (line 5 in Fig. 3) only the plates with thickness $d \geq 0.15 \cdot 50 = 7.5$ nm are enough thick to be considered macroscopically.

IV. INTERACTION OF GRAPHENE WITH A HYDROGEN ATOM OR A MOLECULE

In Sec. II we have described the interaction of graphene with a material semispace by means of the Lifshitz-type formula (1) with the reflection coefficients (3) and (13). This permits us to derive a Lifshitz-type formula for an atom near graphene by considering the limit of rarefied semispace [19, 20]. Let us expand the dielectric permittivity of a semispace in powers of the number of atoms per unit volume N preserving only the first order contribution [19],

$$\varepsilon(i\xi) = 1 + 4\pi\alpha(i\xi)N + \mathrm{O}(N^2), \tag{24}$$

where $\alpha(\omega)$ is the dynamic polarizability of an atom.

Expanding the reflection coefficients (3) and the energy density (1) in powers of N (see Ref. [26] for details), we arrive at the energy of the interaction between an atom and a graphene,

$$E^A(a) = -\frac{\hbar}{2\pi}\int_0^\infty k_\perp dk_\perp \int_0^\infty d\xi\alpha(i\xi)qe^{-2aq} \times \left[2r^{(1)}_{\mathrm{TM,g}} + \frac{\xi^2}{q^2c^2}\left(r^{(1)}_{\mathrm{TE,g}} - r^{(1)}_{\mathrm{TM,g}}\right)\right]. \tag{25}$$

Recall that the reflection coefficients of graphene are given by Eqs. (13).

As was shown in Ref. [18], the atomic and molecular dynamic polarizabilities of H can be represented with sufficient precision using the single oscillator model,

$$\alpha(i\xi) = \alpha_a(i\xi) = \frac{g_a}{\omega_a^2 + \xi^2}, \qquad \alpha(i\xi) = \alpha_m(i\xi) = \frac{g_m}{\omega_m^2 + \xi^2}. \tag{26}$$

Here, $g_a \equiv \alpha_a(0)\omega_a^2$ is expressed through the static atomic polarizability $\alpha_a(0) = 4.50$ a.u. and the characteristic frequency $\omega_a = 11.65$ eV [35]. For a hydrogen molecule $g_m \equiv \alpha_m(0)\omega_m^2$ where $\alpha_m(0) = 5.439$ a.u. and $\omega_m = 14.09$ eV [35]. Note that before the substitution in Eq. (25) the polarizabilities (26) should be expressed in cubic meters taking into account that 1 a.u. of polarizability $= 1.482 \times 10^{-31}\,\mathrm{m}^3$.

For convenience in numerical computations, we introduce the dimensionless variable $y = 2aq$ and represent Eq. (25) in terms of the van der Waals coefficient C_3:

$$E^A(a) = -\frac{C_3(a)}{a^3}, \tag{27}$$

$$C_3(a) = \frac{\hbar}{16\pi}\int_0^\infty dy e^{-y}\int_0^{cy/(2a)} d\xi\alpha(i\xi) \times \left[2y^2 r^{(1)}_{\mathrm{TM,g}} + \frac{4a^2\xi^2}{c^2}\left(r^{(1)}_{\mathrm{TE,g}} - r^{(1)}_{\mathrm{TM,g}}\right)\right].$$

The computational results for C_3 as a function of a obtained by using Eqs. (26) and (27) are presented in Fig. 4. The solid and dashed lines are related to the interaction of graphene with hydrogen atom and molecule, respectively. As is seen in Fig. 4, the magnitudes of the van der Waals coefficient for the hydrogen molecule interacting with graphene are larger than for the atom at all separations. Note that 1 a.u. of $C_3 = 0.646 \times 10^{-48}\,\mathrm{J\,m}^3$. The comparison with the results of Ref. [18] for the interaction of H atoms and molecules with graphite semispace shows that the interaction with graphene is by a factor of more than 2.5 weaker.

V. INTERACTION OF SINGLE-WALL CARBON NANOTUBES WITH METAL OR DIELECTRIC PLATE

Let the single-wall nanotube of radius R lie along the y axis at a separation a from the boundary surface of a material semispace. For sufficiently small a the interaction energy in such configuration can be approximately obtained by using the proximity force theorem [36] and the Lifshitz-type formula (1) for the van der Waals energy between a graphene and a material semispace. According to the proximity force theorem, we replace the cylindrical surface by a set of infinitely long plane strips of width dx. The interaction between each strip, substituting a part of the cylindrical surface, and the opposite strip belonging to the boundary plane of a semispace is calculated by using Eq. (1). The separation distance between the two opposite strips with coordinate x is

$$z = z(x) = a + R - \sqrt{R^2 - x^2}. \tag{28}$$

Expanding the logarithms in Eq. (1) in a power series, we present the interaction energy density between the strips in the form

$$E[z(x)] = -\frac{\hbar}{4\pi^2}\int_0^\infty k_\perp dk_\perp \int_0^\infty d\xi \sum_{n=1}^\infty \frac{1}{n} \times \left[\left(r_{\rm TM}^{(1)} r_{\rm TM}^{(2)}\right)^n + \left(r_{\rm TE}^{(1)} r_{\rm TE}^{(2)}\right)^n\right] e^{-2z(x)qn}. \tag{29}$$

Recall that the reflection coefficients in the case under consideration are given by Eqs. (3) and (13).

To find the interaction energy E^n per unit length between the semispace and the nanotube, we integrate Eq. (29) from $x = -R$ to $x = R$ (this is equal to twice the integral from zero to R). In so doing we replace the variable $k_\perp$ with q from Eq. (2):

$$E^n(a) = -\frac{\hbar}{2\pi^2}\int_0^\infty qdq \int_0^{cq} d\xi \sum_{n=1}^\infty \frac{1}{n} e^{-2aqn} \times \left[\left(r_{\rm TM}^{(1)} r_{\rm TM}^{(2)}\right)^n + \left(r_{\rm TE}^{(1)} r_{\rm TE}^{(2)}\right)^n\right] \int_0^R dx e^{-2qn(R-\sqrt{R^2-x^2})}. \tag{30}$$

By introducing the new variable $s = 1 - \sqrt{1 - x^2/R^2}$, the integral I with respect to x in Eq. (30) can be written in the form

$$I = R\int_0^1 \frac{(1-s)ds}{\sqrt{s(2-s)}} e^{-2qnRs}. \tag{31}$$

The major contribution in Eqs. (30) and (31) comes from $q \sim 1/a$. Bearing in mind that the proximity force theorem works good for $R \gg a$, we conclude that the magnitude of the integral I is determined by the behavior of the integrand around the lower integration limit. Neglecting s compared with unity in Eq. (31), we arrive at

$$I = \frac{R}{\sqrt{2}}\int_0^1 \frac{e^{-2qnRs}}{\sqrt{s}} ds = \frac{1}{2}\sqrt{\frac{\pi R}{qn}}\,{\rm Erf}(\sqrt{2qnR}), \tag{32}$$

where ${\rm Erf}(z)$ is the error function. Using once more the conditions $q \sim 1/a$ and $R \gg a$, we conclude that ${\rm Erf}(\sqrt{2qnR}) \approx 1$ and obtain from Eq. (30)

$$\begin{aligned} E^n(a) &= -\frac{\hbar\sqrt{\pi R}}{4\pi^2}\int_0^\infty \sqrt{q}dq \int_0^{cq} d\xi \sum_{n=1}^\infty \frac{1}{n\sqrt{n}} e^{-2aqn} \\ &\quad \times \left[\left(r_{\rm TM}^{(1)} r_{\rm TM}^{(2)}\right)^n + \left(r_{\rm TE}^{(1)} r_{\rm TE}^{(2)}\right)^n\right] \\ &= -\frac{\hbar\sqrt{R}}{4\pi^{3/2}}\int_0^\infty \sqrt{q}dq \int_0^{cq} d\xi \\ &\quad \times \left[{\rm Li}_{3/2}\left(r_{\rm TM}^{(1)} r_{\rm TM}^{(2)} e^{-2aq}\right) + {\rm Li}_{3/2}\left(r_{\rm TE}^{(1)} r_{\rm TE}^{(2)} e^{-2aq}\right)\right], \end{aligned} \tag{33}$$

where ${\rm Li}_{3/2}(z)$ is the polylogarithm function.

By analogy, for the force per unit length it follows

$$F^n(a)=-\frac{\hbar\sqrt{R}}{2\pi^{3/2}}\int_0^\infty q^{3/2}dq\int_0^{cq}d\xi \times\left[\mathrm{Li}_{1/2}\left(r_{\mathrm{TM}}^{(1)}r_{\mathrm{TM}}^{(2)}e^{-2aq}\right)+\mathrm{Li}_{1/2}\left(r_{\mathrm{TE}}^{(1)}r_{\mathrm{TE}}^{(2)}e^{-2aq}\right)\right]. \tag{34}$$

Note that for an ideal metal cylinder in close proximity to an ideal metal plate the interaction energy and force per unit length are given by [37]

$$E_0^n(a)=-\frac{1}{a^2}\sqrt{\frac{R}{a}}\frac{\pi^3\hbar c}{960\sqrt{2}},\quad F_0^n(a)=-\frac{1}{a^3}\sqrt{\frac{R}{a}}\frac{\pi^3\hbar c}{384\sqrt{2}}. \tag{35}$$

It is significant that Eqs. (33) and (34) follow also in the limit of short separations from the exact result for a nanotube described by the cylindrical surface with the boundary conditions (10) located above a material semispace. This result can be obtained by the method of functional determinants used previously in Refs. [37, 38, 39] for the configurations of a sphere or a cylinder made of ideal metal placed above an ideal metal plate (the details will be published elsewhere). The exact result contains also the asymptotic case of large separations $a\gg R$ between the nanotube and the metal semispace described by the plasma model (18):

$$E^n(a)=\frac{\hbar c}{2\pi a^2\ln\frac{R}{2a}}\int_0^\infty\rho d\rho\frac{\sqrt{\left(\frac{\omega_p a}{c}\right)^2+\rho^2}-\rho}{\sqrt{\left(\frac{\omega_p a}{c}\right)^2+\rho^2}+\rho}\,e^{-2\rho}. \tag{36}$$

This asymptotic behavior does not depend on the nanotube parameter Ω. In the limit $\omega_p\to\infty$ the integral in Eq. (36) tends to 1/4 and we arrive at the previously known result

$$E_0^n(a)=\frac{\hbar c}{8\pi a^2\ln\frac{R}{2a}}, \tag{37}$$

valid for an ideal metal cylinder far away from an ideal metal plate [37, 38].

Now we present the computational results for a nanotube in close proximity and far away from a semispace. Consider, first, the nanotube of radius R in close proximity to Au or Si semispace and compute the normalized interaction energy E^n/E_0^n and the force F^n/F_0^n using Eqs. (33)–(35). As in Sec. III, the dielectric permittivities of Au and Si along the imaginary frequency axis are found from the Kramers-Kronig relations and tabulated optical data for the complex index of refraction. A few computed results are presented in Table II. Column 1 contains the separation distance, columns 2 and 3 contain the values of the correction factor $E^n(a)/E_0^n(a)$ for Au and Si, respectively, and columns 4 and 5 contain the analogous correction factor to the force $F^n(a)/F_0^n(a)$. As is seen in Table II, the magnitudes of all correction factors for Si are smaller than for Au and they are monotonously increasing functions with the increase of separation. Note that the normalized values in Table II do not depend on the nanotube radius. However, bearing in mind that the largest diameter of a single-wall carbon nanotube is of about 10 nm [4], the separation region where the approximate equations (33) and (34) are applicable is very narrow.

Now we consider the nanotube of radius R far away from an Au surface described by the plasma model ($a\gg R$). In this case the Casimir interaction energy is given by Eq. (36). The results of numerical computations of the normalized interaction energy $E^n(a)/E_0^n(a)$, where the energy $E_0^n(a)$ for an ideal metal case is given in Eq. (37), are presented in Fig. 5 as a function of separation. As is seen in Fig. 5, the normalized interaction energy increases with the increase of separation approaching the case of an ideal metal cylinder above an ideal metal plate. At $a=1\,\mu$m it achieves the value of 0.956 very close to the ideal metal case. For the typical single-wall nanotube diameter of about 1 nm the asymptotic expression (36) is applicable in the wide separation region from a few nanometers to about 1 micrometer (for larger separations the thermal corrections should be taken into account).

VI. CONCLUSIONS AND DISCUSSION

In the above we have obtained Lifshitz-type formulas describing the van der Waals and Casimir interaction between graphene and material plate, between an atom or a molecule and graphene, and between a single-wall carbon nanotube and material plate. The distinguishing feature of these formulas is that they describe graphene by using the reflection coefficients obtained from the specific boundary conditions for the electromagnetic oscillations on the infinitely thin plasma sheet. This permits to circumvent the use of the concept of dielectric permittivity commonly used in the Lifshitz

theory of the van der Waals and Casimir force between macrobodies, but being not directly applicable to single-wall carbon nanostructures. The developed formalism is supplementary to widely applied theoretical approaches describing the interactions of carbon nanostructures with macrobodies, atoms or molecules, e.g., to the density functional theory (see Introduction). Together with Ref. [18], where the Lifshitz theory was applied to the multi-wall carbon nanotubes, it provides the foundation for the application of quantum statistical physics to the investigation of dispersion forces in carbon nanostructures.

The obtained Lifshitz-type formulas for the van der Waals and Casimir energy and force were applied to the case of graphene interacting with Au and Si walls. The wall material was described by the dielectric permittivity along the imaginary frequency axis computed using the tabulated optical data for the complex index of refraction for Au and Si. In the case of Au the analytic asymptotic expression for the interaction energy with graphene was also obtained using the plasma model dielectric function. The relationship between the graphene, described by the plasma sheet, and the thin graphite plate was investigated. As an example of microparticle-carbon nanostructure interaction, we have calculated the van der Waals coefficients for the interaction of hydrogen atoms and molecules with graphene. Another example, considered in the paper, is the van der Waals or Casimir interaction of a material wall with a single-wall carbon nanotube in close proximity or far away from the wall, respectively. As was noted in Sec. III, the obtained results for the interaction energy and force are applicable for practical calculations at separations larger than 1–2 nm. At smaller separations there may be the attractive forces of chemical nature. At separations less than 1 nm short-range repulsive forces of exchange nature come into play. These forces depend on atomic structure of a surface and cannot be described macroscopically by means of the boundary conditions. At intermediate separations between the exchange repulsion and van der Waals attraction some phenomenological potentials can be used for practical calculations [41].

In the future work it would be interesting to perform the comparative computations of the van der Waals interaction with carbon nanostructures by using different theoretical approaches. The suggested application of the Lifshitz theory to graphene and single-wall carbon nanotubes can be extended to more complicated structures such as fullerene molecules or graphitic cones [40]. The interaction of hydrogen atoms and molecules with the single-wall carbon nanotubes can be also considered on the same footings. This can be done approximately by using the proximity force theorem because the immediate application of the Lifshitz-type formulas is possible for only planar structures (the results of this work in progress will be published elsewhere). In this paper we did not deal with the thermal effects. However, the generalization of the proposed formalism to the case of nonzero temperatures is straightforward.

Acknowledgments

G. L. K. and V. M. M. are grateful to the Center of Theoretical Studies and the Institute for Theoretical Physics, Leipzig University for their kind hospitality. This work was supported by Deutsche Forschungsgemeinschaft, Grant No. 436 RUS 113/789/0-2. M.B.'s work was supported by the research funding from the ECs Sixth Framework Programme within the STRP project "PARNASS" (NMP4-CT-2005-01707). G. L. K. and V. M. M. were also partially supported by the Russian Foundation for Basic Research (Grant No. 05–08–18119a).

[1] J. Mahanty and B. W. Ninham, *Dispersion Forces* (Academic Press, New York, 1976).
[2] H. B. G. Casimir, Proc. K. Ned. Akad. Wet. **51**, 793 (1948).
[3] H. B. G. Casimir and D. Polder, Phys. Rev. **73**, 360 (1948).
[4] R. Saito, G. Dresselhaus, and M. S. Dresselhaus, *Physical Properties of Carbon Nanotubes* (Imperial College Press, London, 1998).
[5] A. C. Dillon, K. M. Jones, T. A. Bekkedahl, C. H. Kiang, D. S. Bethune, and M. J. Heben, Nature **386**, 377 (1997).
[6] R. G. Ding, G. Q. Lu, Z. F. Yan, and M. A. Wilson, J. of Nanoscience and Nanotech. **1**, 7 (2001).
[7] W. A. Diño, H. Nakanishi, and H. Kasai, e-J. Surf. Sci. Nanotech. **2**, 77 (2004).
[8] I. V. Bondarev and Ph. Lambin, Solid State Commun. **132**, 203 (2004).
[9] I. V. Bondarev and Ph. Lambin, Phys. Rev. B **72**, 035451 (2005).
[10] Ch. Girard, Ph. Lambin, A. Dereux, and A. A. Lucas, Phys. Rev. B **49**, 11425 (1994).
[11] A. Bogicevic, S. Ovesson, P. Hyldgaard, B. I. Lundqvist, H. Brune, and D. R. Jennison, Phys. Rev. Lett. **85**, 1910 (2000).
[12] E. Hult, P. Hyldgaard, and B. I. Lundqvist, Phys. Rev. B **64**, 195414 (2001).
[13] H. Rydberg, M. Dion, N. Jacobson, E. Schröder, P. Hyldgaard, S. I. Simak, D. C. Landreth, and B. I. Lundqvist, Phys. Rev. Lett. **91**, 126402 (2003).
[14] J. Jung, P. García-González, J. F. Dobson, and R. W. Godby, Phys. Rev. B **70**, 205107 (2004).
[15] J. Kleis, P. Hyldgaard, and E. Schröder, Comp. Mat. Sci. **33**, 192 (2005).
[16] J. F. Dobson, A. White, and A. Rubio, Phys. Rev. Lett. **96**, 073201 (2006).

[17] L. A. Girifalco and M. Hodak, Phys. Rev. B **65**, 125404 (2002).
[18] E. V. Blagov, G. L. Klimchitskaya, and V. M. Mostepanenko, Phys. Rev. B **71**, 235401 (2005).
[19] E. M. Lifshitz, Zh. Eksp. Teor. Fiz. **29**, 94 (1956) [Sov. Phys. JETP **2**, 73 (1956)].
[20] E. M. Lifshitz and L. P. Pitaevskii, *Statistical Physics* (Pergamon Press, Oxford, 1980), Pt. II.
[21] M. Bordag, U. Mohideen, and V. M. Mostepanenko, Phys. Rep. **353**, 1 (2001).
[22] F. Chen, U. Mohideen, G. L. Klimchitskaya, and V. M. Mostepanenko, Phys. Rev. Lett. **88**, 101801 (2002); Phys. Rev. A **66**, 032113 (2002).
[23] R. S. Decca, E. Fischbach, G. L. Klimchitskaya, D. E. Krause, D. López, and V. M. Mostepanenko, Phys. Rev. D **68**, 116003 (2003).
[24] F. Chen, G. L. Klimchitskaya, U. Mohideen, and V. M. Mostepanenko, Phys. Rev. A **69**, 022117 (2004).
[25] F. Chen, U. Mohideen, G. L. Klimchitskaya, and V. M. Mostepanenko, Phys. Rev. A **72**, 020101(R) (2005); **74**, 022103 (2006).
[26] J. F. Babb, G. L. Klimchitskaya, and V. M. Mostepanenko, Phys. Rev. A **70**, 042901 (2004).
[27] M. Antezza, L. P. Pitaevskii, and S. Stringari, Phys. Rev. A **70**, 053619 (2004).
[28] A. L. Fetter, Ann. Phys. (N.Y.) **81**, 367 (1973).
[29] G. Barton, J. Phys. A: Math. Gen. **37**, 1011 (2004).
[30] G. Barton, J. Phys. A: Math. Gen. **38**, 2997 (2005).
[31] M. Bordag, J. Phys. A: Math. Gen. **39**, 6173 (2006).
[32] G. A. Gallup, Chem. Phys. Lett. **187**, 187 (1991).
[33] A. O. Caride, G. L. Klimchitskaya, V. M. Mostepanenko, and S. I. Zanette, Phys. Rev. A **71**, 042901 (2005).
[34] *Handbook of Optical Constants of Solids*, ed. E. D. Palik (Academic Press, New York, 1985).
[35] A. Rauber, J. R. Klein, M. W. Cole, and L. W. Bruch, Surf. Sci. **123**, 173 (1982).
[36] J. Blocki, J. Randrup, W. J. Swiatecki, and C. F. Tsang, Ann. Phys. (N.Y.) **105**, 427 (1977).
[37] M. Bordag, Phys. Rev. D **73**, 125018 (2006).
[38] T. Emig, R. L. Jaffe, M. Kardar, and A. Scardicchio, Phys. Rev. Lett. **96**, 080403 (2006).
[39] A. Bulgac, P. Magierski, and A. Wirzba, Phys. Rev. D **73**, 025007 (2006).
[40] P. E. Lammert and V. H. Crespi, Phys. Rev. Lett. **85**, 5190 (2000); Phys. Rev. B **69**, 035406 (2004).
[41] J. Israelachvili, *Intermolecular and Surface Forces* (Academic Press, New York, 1992).

Figures

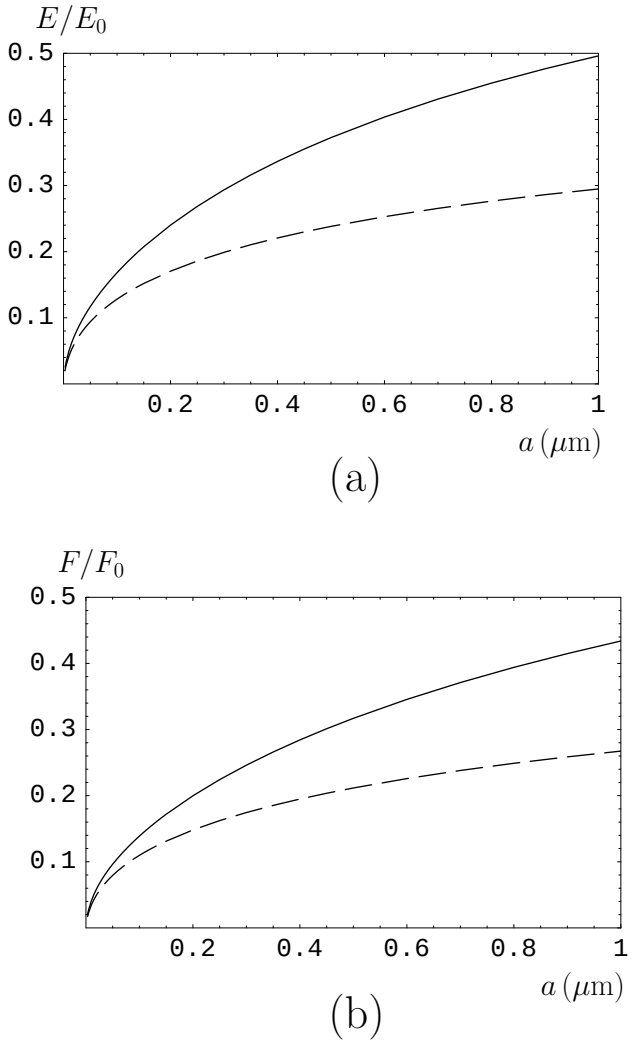

FIG. 1: The normalized to the case of ideal metals van der Waals and Casimir energy (a) and force (b) per unit area between a graphene and a semispace versus separation. The solid and dashed lines are related to the semispace made of Au and Si, respectively.

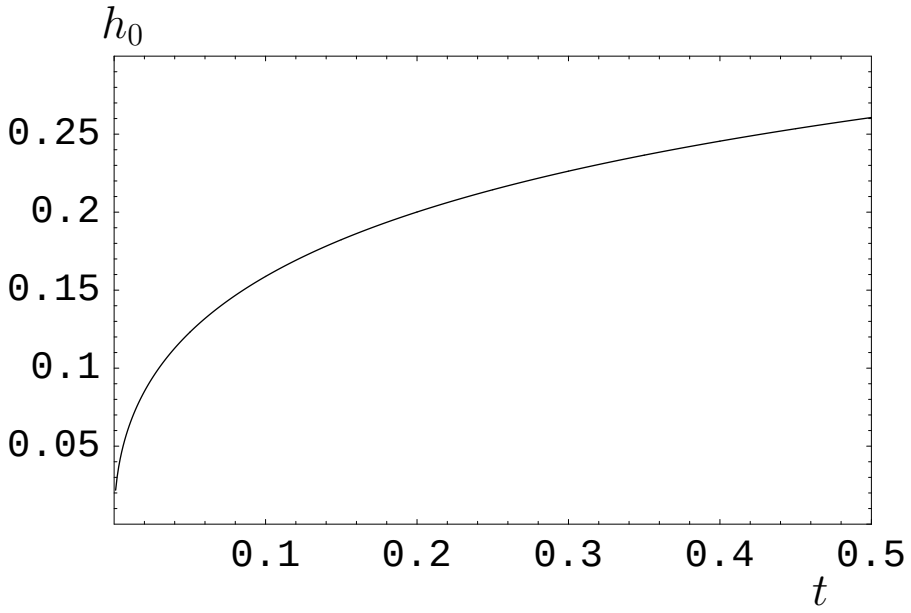

FIG. 2: The function h_0 in Eq. (21) versus the dimensionless parameter $t = \Omega c^2/(\omega_p^2 a)$.

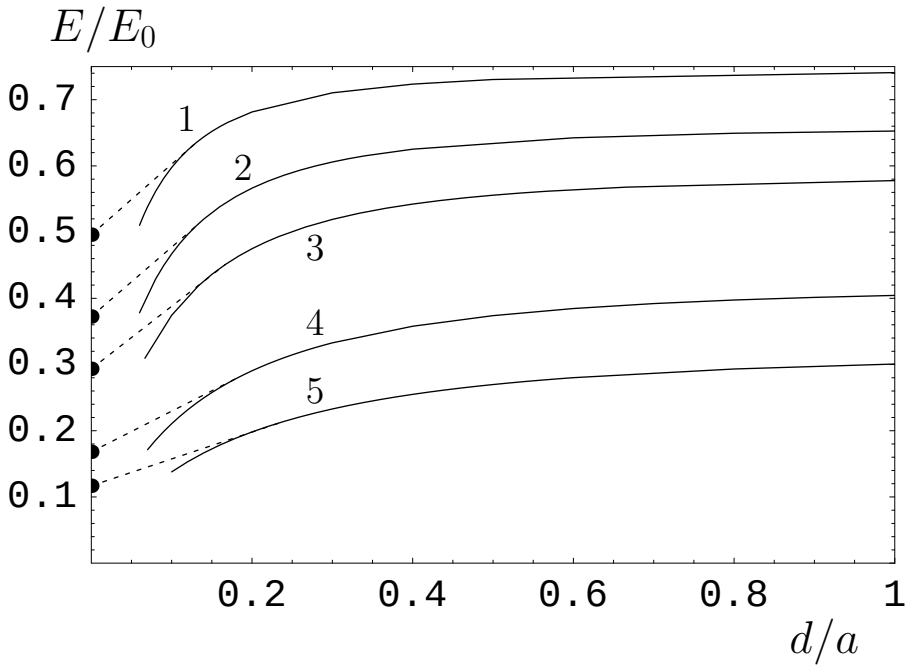

FIG. 3: The normalized to the case of ideal metals van der Waals and Casimir energy per unit area between a graphite plate of thickness d and Au semispace versus relative thickness. Lines $1, 2, 3, 4$, and 5 are related to separations $a = 1$, 0.5, 0.3, 0.1, and $0.05\,\mu$m, respectively. The respective normalized interaction energies of a graphene with an Au semispace are marked on the vertical axis (see text for further discussion).

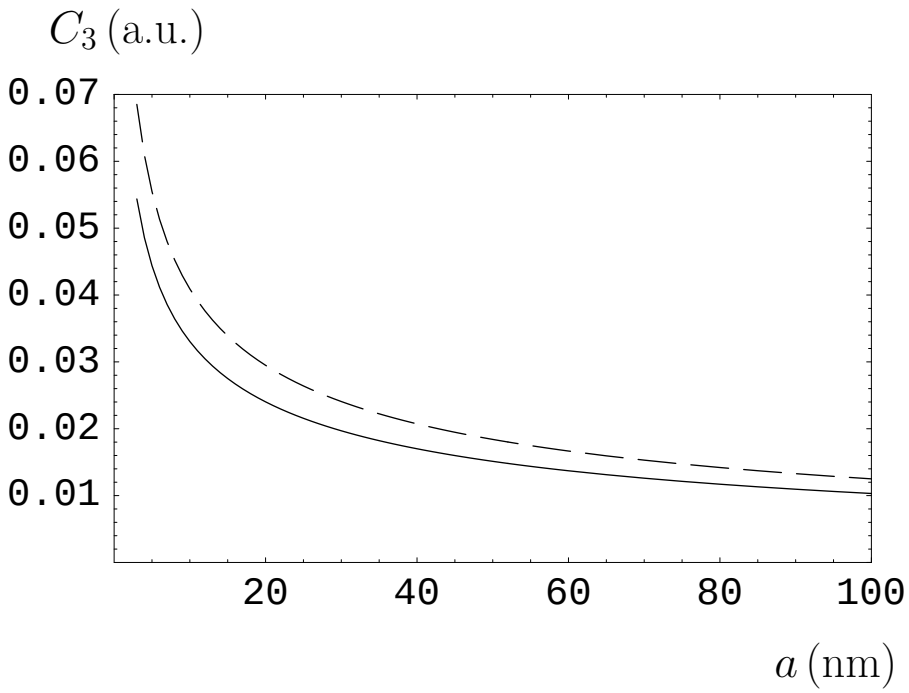

FIG. 4: The van der Waals coefficient C_3 for the interaction of a hydrogen atom (the solid line) and a molecule (the dashed line) with graphene versus separation.

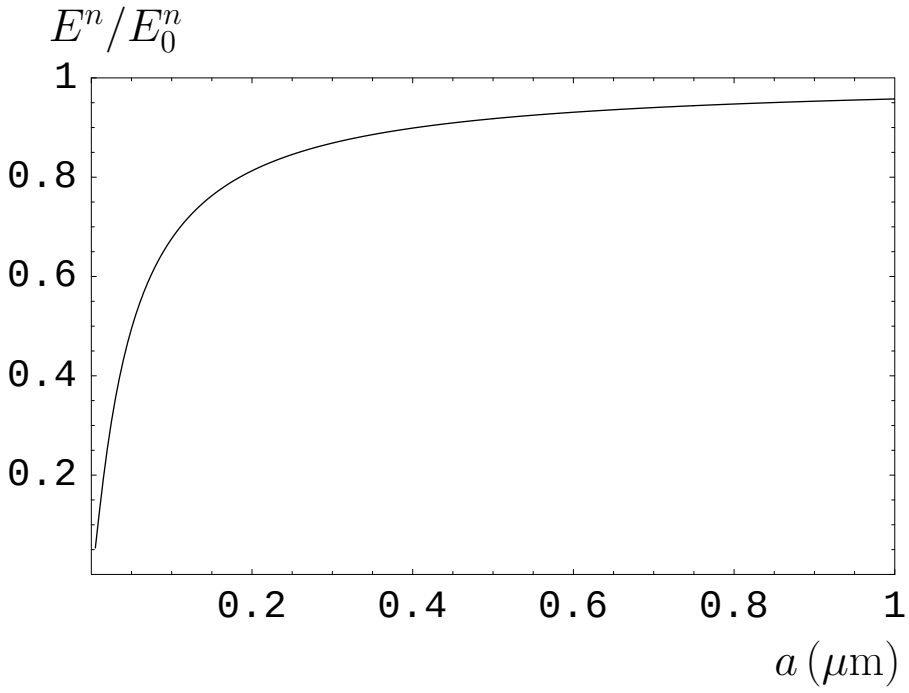

FIG. 5: The normalized to the case of ideal metals Casimir energy per unit length between a carbon nanotube and Au semispace versus separation.

Tables

TABLE I: Ratios $E(a)/E_0(a)$ for the Casimir interaction of an Au semispace and graphene computed using: (a) — tabulated optical data for Au, (b) — plasma model for Au, (c) — asymptotic expression (23).

a	$E(a)/E_0(a)$		
(nm)	(a)	(b)	(c)
3	0.0252	0.0222	0.0223
5	0.0338	0.0307	0.0310
10	0.0496	0.0466	0.0473
15	0.0618	0.0590	0.0602
20	0.0720	0.0694	0.0711
30	0.0893	0.0870	0.0895
40	0.104	0.102	0.105
50	0.117	0.115	0.119
60	0.129	0.127	0.131
70	0.139	0.138	0.143
80	0.1496	0.1485	0.154

TABLE II: Ratios $E^n(a)/E_0^n(a)$ and $F^n(a)/F_0^n(a)$ for the van der Waals interaction of a carbon nanotube with Au and Si semispaces

a	$E^n(a)/E_0^n(a)$		$F^n(a)/F_0^n(a)$	
(nm)	Au	Si	Au	Si
1	0.0151	0.0126	0.0114	0.00945
1.5	0.0193	0.0162	0.0147	0.0123
2	0.0230	0.0193	0.0175	0.0147
2.5	0.0262	0.0221	0.0201	0.0169
3	0.0291	0.0245	0.0224	0.0189